Design Wave Elevations Leading to Extreme Roll Motion

Laura K. Alford*, Armin W. Troesch†, Leigh S. McCue‡

Abstract

Response-tailored wave trains are created for use in numerical capsize experiments. The wave trains are tailored to produce a specified, linear, large response by considering the statistical distribution of the response phases in the neighborhood of a typical maximum response. The statistical distribution is seen to be *non*-uniform. Using a non-uniform distribution for the random phases, design wave elevations leading to extreme rolling are created for a box barge and used as input to a nonlinear seakeeping code. Several wave trains also designed to lead to extreme rolling are produced for a high speed containership for a range of conditions.

1 Introduction

The study of extreme waves has been going on in the marine industry for many years, but only relatively recently has the focus been on extreme responses of floating structures. An extreme response was generally held to be the result of an encounter with an exceptionally large wave. This large wave may be elusive and usually only found in long numerical simulations of the ocean's surface during a storm. Trying to find it by generating a random sea in a towing tank is difficult; model basins are generally not of sufficient size to allow the entire sea to be generated before wave reflection becomes an issue. The logical conclusion: find a wave sequence leading to extreme responses in a very short period of time, both in the tank and numerically.

Davis and Zarnick (1964) initiated current interest by using the linear dispersion relation to focus experimentally and force them to all reach the same point at the same time, resulting in a large wave crest. Others - including Takezawa and Takekawa (1976), Takezawa and Hirayama (1976), Clauss and Bergmann (1986) and Chakrabarti and Libby (1988) - followed in their footsteps and refined the procedure. The number of different crests that could be produced was greatly expanded, but which one was "correct?" Hoping to answer that question, Tromans et. al. (1991) devised a method for predicting the shape of the most likely extreme wave in the immediate vicinity of that same peak. This method is based on linear, broad-banded wave theory and uses probability theory to find the expected value of the wave shape given that at time t_1, $\eta(x_1, y_1, t_1) = \alpha$ and $\dot{\eta}(x_1, y_1, t_1) = 0$. The method assumes that, at a large crest, all the component waves are either in phase or out of phase. Taylor et. al. (1995) inserted the known maximum wave crest into any conventionally created random wave train, thus giving the designer the option of producing a more extended irregular wave record.

Another approach to tailoring waves was presented by Steinhagen (2001). Steinhagen uses the Sequential Quadratic Programming method to optimize the phases associated with an initial random wave train such that the result is the desired extreme waves. Parameters in the optimization include: matching the target wave height, the wavelength of the extreme wave, the maximum crest height, the time of the extreme height, and wavemaker constraints while keeping the phases between $-\pi$ and π. The result, after the optimization routine has run, are the new phases to be used with their respective wave components. This approach was used quite successfully by Clauss (2002) and Clauss et. al. (2004) in creating the wave train at the wavemaker that results in an extreme wave down-tank. A nonlinear marching technique was then employed to determine the true shape of the wave train down-tank, and this wave train was then used in subsequent numerical experiments.

These approaches are straightforward and easy to understand but deal solely with the waves. The response to an extreme wave is still a reasonable prediction of design loads for structures such as offshore platforms since the response is driven primarily by hydrostatic changes. However, for dynamic, moving ships there is no guarantee that the extreme response occurs with the extreme wave.

*Naval Architecture and Marine Engineering, University of Michigan, lslavice@engin.umich.edu

†Naval Architecture and Marine Engineering, University of Michigan

‡Aerospace and Ocean Engineering, Virgina Tech

Adegeest et. al. (1998) took the natural step of applying Tromans' method to finding the shape of the most likely extreme *response*. The amplitudes and phases of the incident wave components could then be back-computed via linear theory, giving the tailored wave shape near the desired crest. Similarly, Clauss et. al. (2003) used the roll response spectrum of the ship to further tailor the waves according to Clauss (2002). Additionally, Clauss et. al. (2004) investigated the reactions of a ship to a rogue wave, particularly as it relates to capsize.

This paper investigates a third approach to the creation of extreme waves leading to design response: using a non-uniform distribution for the random phases associated with the component waves.

2 Background

This work employs Fast Fourier Transforms (FFTs). In the creation of random waves, the FFT allows the engineer to not only quickly create a random space-time series, but to shift it in time or space with simple phase adjustments. With regard to phase adjustments, the following sections describe the most common wave model as well as the authors' proposed new wave model.

2.1 The Usual Wave Model

Assuming stationarity and ergodicity of the ocean for a short period of time, one may represent the ocean surface at some point (x, y) as the summation of many component waves:

$$\zeta(x, y, t) = \sum_{j=1}^{N} a_j \cos(\omega_j t + \beta_j) \tag{1}$$

$\zeta(x, y, t)$	wave elevation
N	number of components
a_j	amplitude of jth component
ω_j	frequency of jth component
β_j	phase of jth component

The amplitudes and frequencies are determined by the spectrum (e.g. Pierson-Moskowitz, ITTC, Ochi 8-parameter, etc.) that will characterize the time series. The randomness enters through the phases, which are chosen from a uniform distribution between $-\pi$ and π. At each time step, the components are summed for the current t value and the wave elevation recorded. For large N, this straightforward summation becomes computationally expensive; however, it may be noted that Equation 1 is equivalent to the real part of the complex inverse FFT (IFFT) where the Fourier Transform of the ocean surface is defined by a_j and β_j. Using the IFFT to directly transfer between frequency and time domain saves on computation time and also allows the designer to calculate the ocean surface in space if x and y are allowed to vary in Equation 1. When using the IFFT to do this summation, the number of components is determined by the time step and the length of the resulting time series.

$$N = T_{record}/\Delta t \tag{2}$$

For large N, zero padding is commonly employed, and the non-zero amplitudes are limited to the frequency range of the input spectrum. With the frequency step inversely dependent on the record length,

$$\Delta\omega = \frac{2\pi}{T_{record}} \tag{3}$$

it is clear that the number of non-zero components can vary drastically based solely on the length of the time series. This is a cause for concern because the usual assumption is that the ocean surface may represented by the sum of many components, not a few. Fortunately, for a given Δt, a reasonable approximation of the water surface may be obtained with a relatively finite number of components (i.e. a short time series) and the issue then becomes the determination of the phases. The two primary methods presented in Section 1 determine wave phases producing a specific wave shape, but in doing so create a deterministic process. The model presented below attempts to keep the stochastic nature of the problem.

2.2 A New Wave Model

Consider now, a slight adjustment to the above model, Equation 1. Shift the time series so that the maximum crest occurs at zero:

$$\zeta(x, y, t') = \sum_{j=1}^{N} a_j \cos(\omega_j t' + \beta_j) \tag{4}$$

t'	$= t - t_{max}$
t_{max}	time of maximum crest

This can be rewritten as,

$$\zeta(x, y, t') = \sum_{j=1}^{N} a_j \cos(\omega_j(t - t_{max}) + \beta_j) \quad (5)$$

$$= \sum_{j=1}^{N} a_j \cos(\omega_j t - \omega_j t_{max} + \beta_j) \quad (6)$$

$$= \sum_{j=1}^{N} a_j \cos(\omega_j t + \beta'_j) \quad (7)$$

Where the new phases are

$$\beta'_j = \beta_j - \omega_j t_{max} \quad (8)$$

When a long time record is considered, the β'_js are still uniformly distributed, as each new phase is simply the original phase with a constant parameter subtracted from it. At the large crest, the β'_js are distributed in such a way that a sufficient number of wave components are in phase to produce the given crest height. In the limit of an infinite number of wave phases and a finite crest, the distribution is uniform as the crest can be made by summing only a small proportion of the available components. However, when the number drops significantly, such as would happen when one IFFTs to simulate a short time series of 120 seconds, the phases are forced out of their uniform distribution to make up for the sudden lack of flexibility.

Figures 1 and 2 show a sample of one of 10 very long records produced according to Equation 1, with a_j and ω_j being determined by an ITTC spectrum with a significant height of 2.89 ft (0.88m) and peak period of 7.5 seconds. Each long time series is 104,857.6 seconds long and used 1,048,576 points in the inverse FFT, 37,850 of which had non-zero amplitudes. An estimation of the probability density function (PDF) of each long time series was determined by a phase histogram and the 10 histograms combined to form an ensemble average. The phases are uniformly distributed as can be seen in the left graph of Figure 2. Each record was then scanned and the absolute maximum found. A separate, short time series was created that was centered about that maximum value and duly FFT'd. The PDFs of the phases of the 10 runs were determined as just described, combined, and resulted in the right hand graph of Figure 2.

The resulting phase distribution of the short time series depends on many factors including:

- the crest height, especially as relates to the RMS of the process (a measure of how extreme the event is)
- the number of components and, by Equation 3, the length of the short record

A cursory examination of the new phase distribution shows peaks at both 0 (crests) and $\pm\pi$ (troughs); this is logical when one considers that large peaks generally occur with large troughs. The only remaining step in the process is to apply this formulation to the response spectrum instead of the wave spectrum, back-compute the incident wave according to linear theory, and the result will be response-tailored waves suitable for investigating anything from a design midship bending moment to extreme roll. The advantage of this method is that nowhere has the wave shape been constrained other than to produce a large response. The wave train leading to the extreme event could be a single, large wave as in Tromans' or Steinhagen's work, or it could be a group of waves travelling together.

3 Application: Leading to Extreme Rolling

The method used for this paper takes a simplified approach and assumes a zero-mean, Gaussian distribution with a given standard deviation for the phases. The standard deviation is chosen by the user to give the phases a distribution such that a given, maximum, linear response is reached - the Target Extreme Value (TEV). The TEV is defined in relation to the root mean square (RMS) of the process, thereby building in a measure of the extremity of the event. The result is a truncated Gaussian distribution with a mean of zero and bounded by $-\pi$ and π.

3.1 Selection of Target Extreme Value

Freak waves are often initially classified as being 2-2.5 times the local significant wave height. The significant wave height is defined as

$$\bar{h}_{1/3} = 4.0\sigma_{wave} \quad (9)$$

where σ_{wave} is the RMS of the random waves. If the crest height is used as the extreme value, then the TEV could have a range of

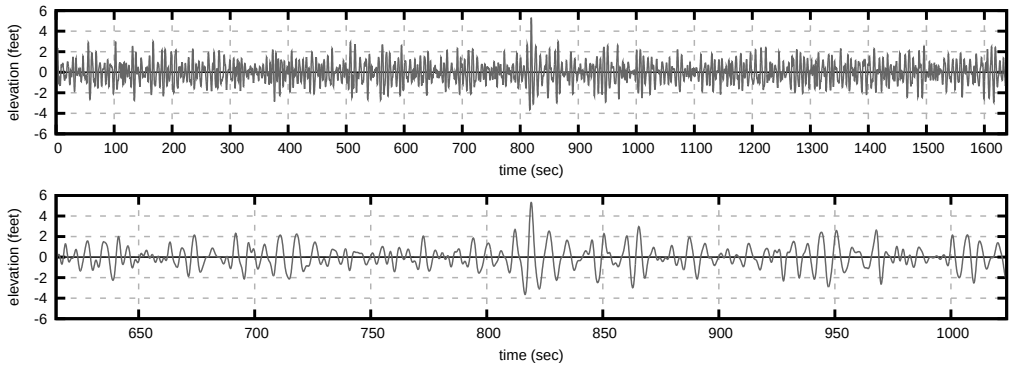

Figure 1: A randomly created time series. *Top:* A portion of a very long time series, centered around the maximum of the series; the total length of the generated time series is 104857.6 seconds, $\Delta t = 0.1$ seconds, N = 1048576 for Fourier Transform, 37850 non-zero components. The portion shown here has a total length of 1638.4 seconds, $\Delta t = 0.1$ seconds, N = 16384 for Fourier Transform, 1184 non-zero components; this time series is the source of the phase distribution in the right hand graph of Figure 2. *Bottom:* A closer look at the maximum value of the top series.

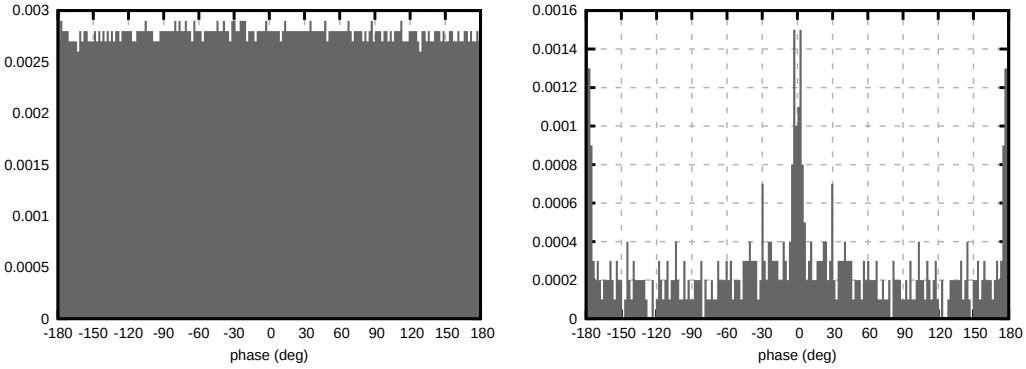

Figure 2: Phase distributions of two types of time series. *Left:* The combined phase distribution for 10 very long time series; T = 104,857.6 seconds, $\Delta t =$ 0.1 seconds, N = 1,048,576 for each series. This phase distribution considers only the non-zero components, a total of 378,500 for the 10 time series, and is characteristic of the very long time series of which Figure 1 shows a portion. *Right:* The combined phase distribution for a short time series centered about the maximum of each long time series; T = 1638.4 seconds, $\Delta t = 0.1$ seconds, N = 16384 for each time series. This phase distribution considers only the non-zero components, a total of 11,840 for the 10 time series, and is characteristic of the top series in Figure 1.

$$2\frac{\bar{h}_{1/3}}{2} \leq TEV \leq 2.5\frac{\bar{h}_{1/3}}{2} \quad (10)$$

$$2\frac{4.0\sigma_{wave}}{2} \leq TEV \leq 2.5\frac{4.0\sigma_{wave}}{2} \quad (11)$$

$$4.0\sigma_{wave} \leq TEV \leq 5.0\sigma_{wave} \quad (12)$$

For a general process with an RMS of σ and following a Rayleigh PDF, the most probable 1/Nth largest response is

$$\bar{\zeta}_{1/N} = \sigma\sqrt{2.0 \ln N} \quad (13)$$

where N = number of wave encounters. Assigning a TEV to $\bar{\zeta}_{1/N}$ and rearranging to solve for N yields

$$N = e^{\left(\frac{1}{2}\left(\frac{TEV}{\sigma}\right)^2\right)} \quad (14)$$

For example, choosing a TEV of 4.4σ results in $N \approx 268,000$; in other words, this TEV has a probability of 1/268,000 of occurring.

3.2 Box Barge

To illustrate this method, a design wave elevation leading to extreme roll was produced for a box barge and used in a 3 degree of freedom quasi-nonlinear code to determine extreme responses in beam seas. The code and barge (length 66.1m, beam of 12.2m, draft of 3.0m, with 0.3m freeboard and an angle of vanishing stability of 31.7°) used are the same as those used in McCue and Troesch (2005). Details of the quasi-nonlinear simulation can be found in Lee et al. Additionally, the numerical code was modified to include random waves.

The TEV chosen was 2.89°, the angle when the deck first wets and linear analysis loses accuracy. Using the 4.4σ measure of an extreme event from Section 3.1, the needed RMS of roll is found by

$$\sigma_{roll} = \frac{2.89^\circ}{4.4} = 0.6568^\circ \quad (15)$$

The box barge was analyzed using the linear seakeeping code SHIPMO (Beck and Troesch (1990)) to match σ_{roll} in beam seas for zero forward speed with an ITTC spectrum. The resulting spectrum had a significant wave height of 0.277m and peak period of 7.5s. Using the Response Amplitude Operators (RAOs) of the 6 degree of freedom system output by SHIPMO, the roll response spectrum for the barge was calculated by linear theory with the complex roll RAO $H_{roll}(\omega)$,

$$S^+_{roll}(\omega) = |H_{roll}(\omega)|^2 S^+_{wave}(\omega) \quad (16)$$

Using the roll response spectrum to determine the amplitudes associated with each frequency component, a design response time series was generated according to Equation 5 and utilizing the IFFT with 201 non-zero components. The 120-second time series used a standard deviation of 60° for the random phase distribution and a phase shift of $-\omega_j t_{crit}$ to put the maximum value at $t_{crit} = 60$ seconds. The corresponding incident wave train was back calculated by,

$$\zeta(t) = \sum_{j=1}^{N} \zeta_j \cos(\omega_j t + \alpha_j) \quad (17)$$

$$\zeta_j = \frac{a_j}{|H_{roll}(\omega_j)|} \quad (18)$$

$$\alpha_j = \beta'_j - \phi_j \quad (19)$$

where a_j and β'_j are now associated with the *response* spectrum and ϕ_j are the corresponding phases for each frequency component in the roll RAO.

The wave train was then given to the nonlinear code for analysis. Taking advantage of linear superposition, several incident wave trains were created by scaling the original amplitudes by a given factor until capsize occurred. Each train retains its characteristics that lead to extreme roll, but the nonlinearities become more pronounced as the amplitudes increase. Figure 3 demonstrates the differences between the linear predicted response (itself scalable) to the non-scaled wave train and the successive nonlinear responses.

The inclusion of sway effects in the nonlinear code accounts for the shift of the maximum roll away from t_{crit}. Also, the nonlinear responses do not damp out as quickly after the large roll is experienced as the linear response, as to be expected from the weakening of the restoring force at higher angles. The barge appears to be particularly sensitive to a large, single wave under these conditions. As the incident wave train is scaled up, the barge's response becomes increasingly irregular, ultimately resulting in capsize.

3.3 High Speed Containership

As an additional example, design wave elevations aimed at producing extreme roll motions for a range of conditions for a high speed containership, model SR-175, were created. SR-175 has a length, beam, and draft of 175m, 25.4m, and 9.5m respectively with a block coefficient of 0.5694.

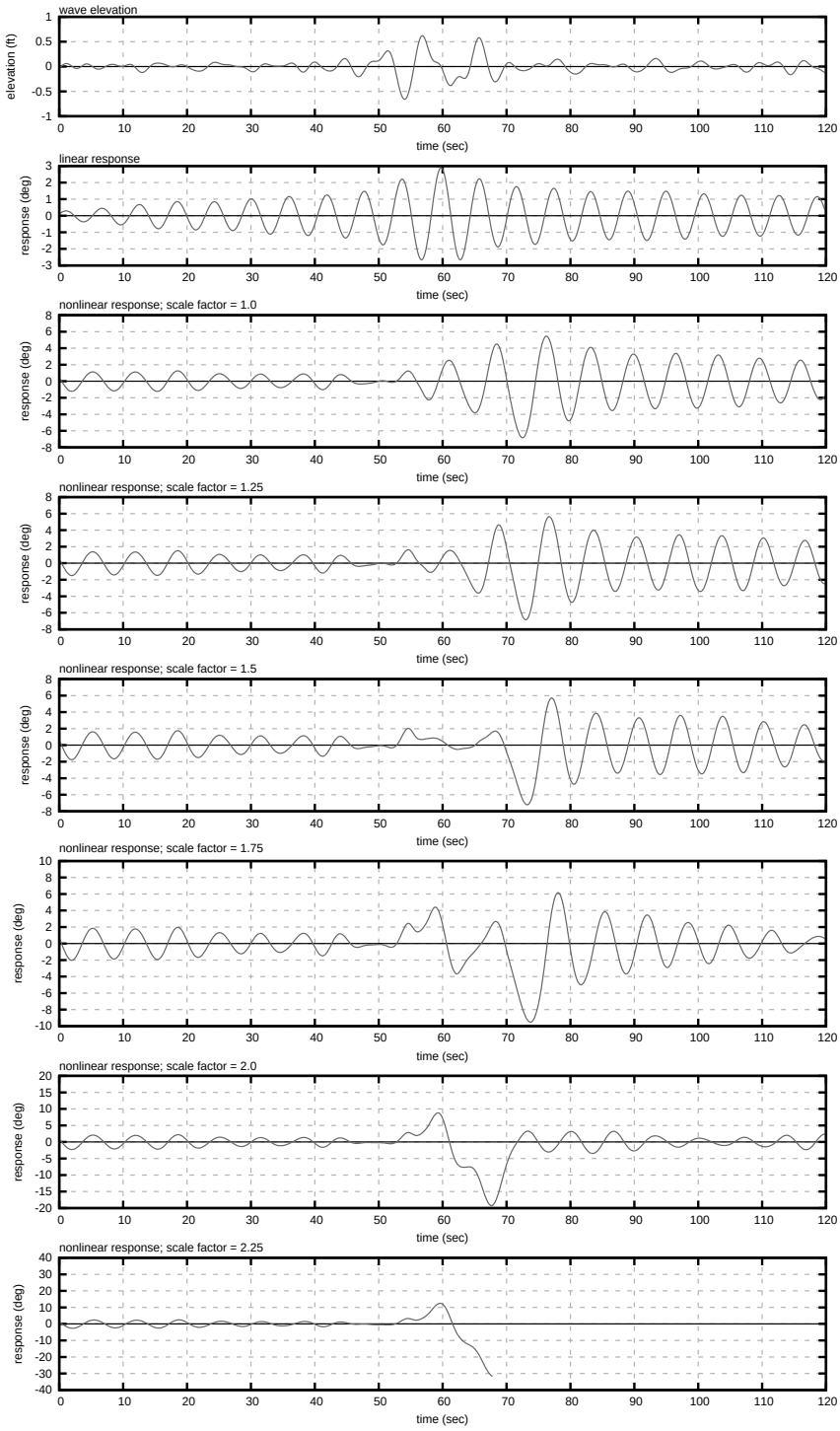

Figure 3: Linear vs. nonlinear design roll motion for a box barge in beam seas, $V_k = 0$ kts. The first graph is the linear design wave train that produces the linear response in the next graph. The subsequent 6 graphs show the nonlinear results as the linear wave train is increasingly scaled. Capsize occurs for a scale factor of 2.25. 201 non-zero components were used for each time series.

Experiment #	V_k (kts)	θ (deg)	$h_{sig.}$ (m)	T_p (sec)	σ_{roll} (deg)	$TEV = 4.4\sigma_{roll}$ (deg)	phase std. dev. (deg)
1	0	135	3.25	9.7	0.550	2.42	75
2	0	90	3.25	9.7	0.265	1.17	75
3	0	45	3.25	9.7	0.466	2.05	75
4	20	135	3.25	9.7	0.215	0.946	75
5	20	90	3.25	9.7	0.270	1.19	75
6	20	45	3.25	9.7	8.510	37.4	75

Table 1: Experiment parameter space for SR-175 model high speed containership. θ = heading angle; 180° is head seas. σ_{roll} is the RMS of roll obtained from linear theory. TEV = Target Extreme Value. Phase standard deviation is the standard deviation used to define the Gaussian distribution of the phases in Equation 7. Each time simulation is 120 seconds long with the maximum focused at 60 seconds except for experiment 6 which is 300 seconds long with the maximum at 150 seconds.

The matrix for the numerical experiments is shown in Table 1. The same TEV of $4.4\sigma_{roll}$ was used, but now σ_{roll} is dictated by the sea states in Table 1. The time series used a standard deviation of 75° for the random phase distribution and t_{crit} = 60 seconds (150 seconds for experiment 6). The results of the 6 experiments are shown in Figures 4 - 9. A number of observations immediately arise:

- The equivalent TEV for the sea state used in each experiment is 3.58 meters. Only in experiment 5 (V_k = 20 kts, beam seas) does a wave reach that crest value, yet each response is, by its own definition, extreme for the conditions.
- The method is able to produce a range of extreme motions due to the linear nature of the initial estimation of the design wave elevation. Anything from a tiny TEV of 0.946° for V_k = 20 kts, bow quartering seas to a much more concerning 37.4° for V_k = 20 kts, stern quartering seas.
- There is a poignant difference in the types of waves that generate large responses. This method captures both a single large wave, such as in experiment 5, or a group of waves, as in experiment 6. Both produce extreme responses.

4 Conclusions

The method just presented is a fast, efficient way to predict a design wave elevation leading to extreme responses from linear theory. It is quite flexible both to the input extreme value and the type of waves produced. The method can easily be applied to any process that can be described linearly, such as bending moment or acceleration at the bridge, and possibly even be an indicator of some types of nonlinear behavior. For example, a design wave elevation that leads to severe relative velocity between the bow and the water surface in the linear world may produce severe slamming loads in the nonlinear world.

Current research includes determining the relationship between the PDF of the phases around a maximum or minimum and possible input parameters. Continuing work on integrating the method with other nonlinear seakeeping codes and optimization codes is also being done.

5 Acknowledgments

The work in this paper was partially supported by the National Defense Science and Engineering Graduate Fellowship and the Department of Naval Architecture and Marine Engineering, University of Michigan. The authors also wish to thank Dr. Young-Woo Lee for his work in the development of the quasi-nonlinear capsize code.

References

[1] L. Adegeest, A. Braathen, and R. M. Løseth. Use of non-linear sea-loads simulations in design of ships. *Proc. Practical Design of Ships and Mobile Units (PRADS)*, pages 53–58, 1998.

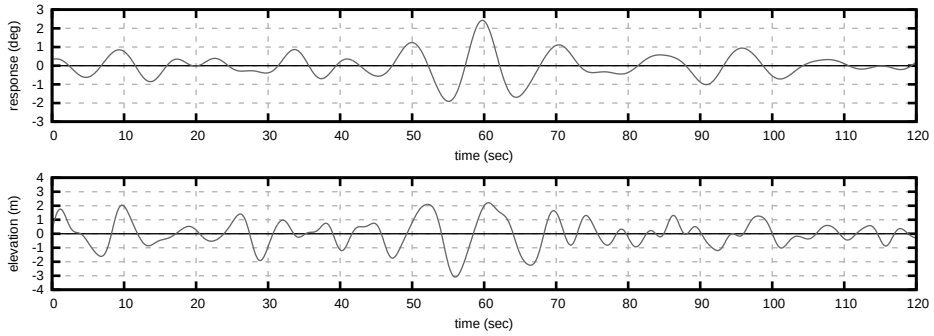

Figure 4: Experiment 1. Design roll motion; $V_k = 0$ kts, bow quartering seas. *Top:* Roll response of ship, TEV = 2.42°. *Bottom:* The design wave train computed to produce an extreme roll angle.

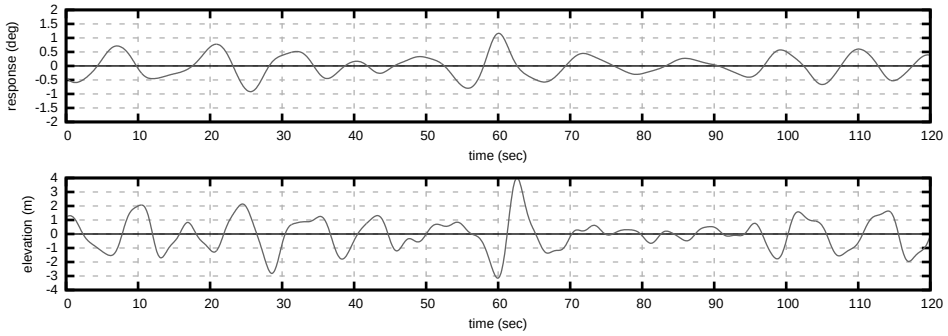

Figure 5: Experiment 2. Design roll motion; $V_k = 0$ kts, beam seas. *Top:* Roll response of ship, TEV = 1.17°. *Bottom:* The design wave train computed to produce an extreme roll angle.

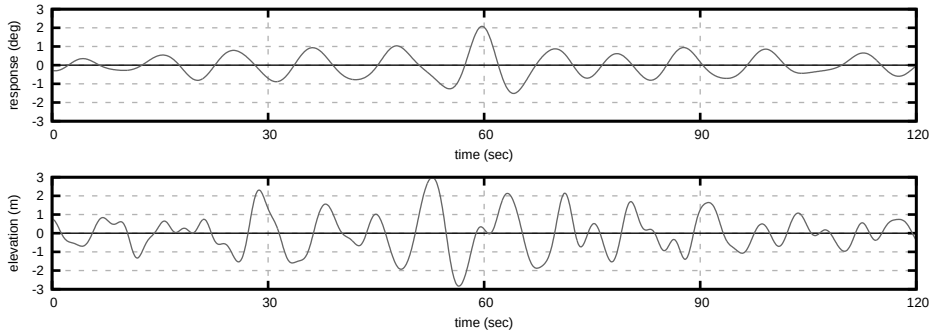

Figure 6: Experiment 3. Design roll motion; $V_k = 0$ kts, stern quartering seas. *Top:* Roll response of ship, TEV = 2.05°. *Bottom:* The design wave train computed to produce an extreme roll angle.

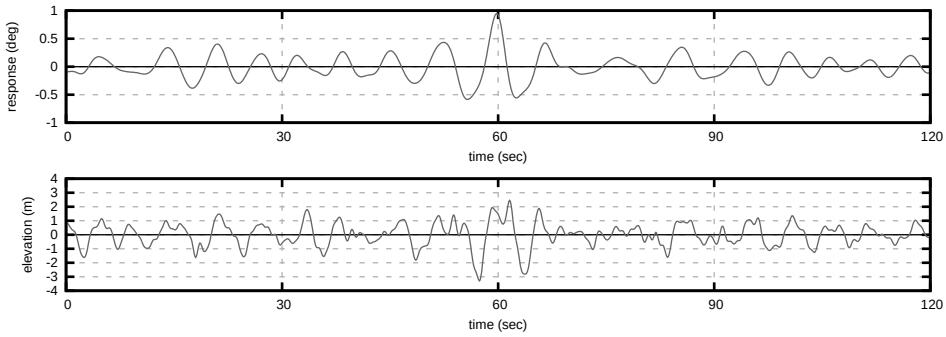

Figure 7: Experiment 4. Design roll motion; $V_k = 20$ kts, bow quartering seas. *Top:* Roll response of ship, TEV = 0.946°. *Bottom:* The design wave train computed to produce an extreme roll angle.

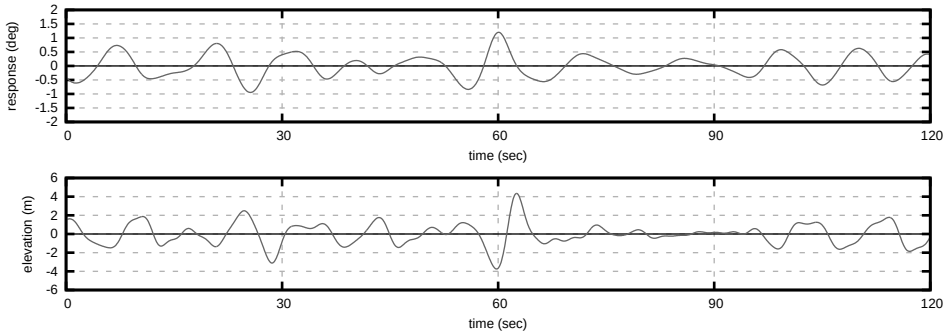

Figure 8: Experiment 5. Design roll motion; $V_k = 20$ kts, beam seas. *Top:* Roll response of ship, TEV = 1.19°. *Bottom:* The design wave train computed to produce an extreme roll angle.

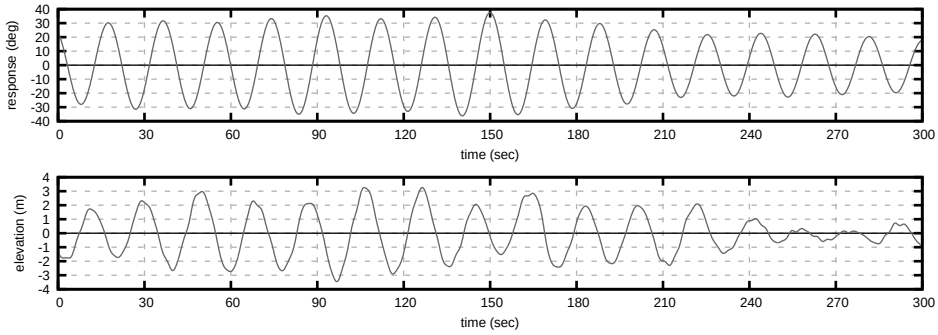

Figure 9: Experiment 6. Design roll motion; $V_k = 20$ kts, stern quartering seas. *Top:* Roll response of ship, TEV = 37.4°. *Bottom:* The design wave train computed to produce an extreme roll angle.

[2] L. Adegeest, A. Braathen, and T. Vada. Evaluation of methods for estimation of extreme nonlinear ship responses based on numerical simulations and model tests. *Proc. Twenty-Second Symposium on Naval Hydrodynamics*, pages 84–99, 1999.

[3] R. F. Beck and A. W. Troesch. *Students documentation and users manual for the computer program SHIPMO.BM.* Department of Naval Architecture and Marine Engineering, University of Michigan, Ann Arbor, 1990.

[4] S. Chakrabarti and A. Libby. Further verification of gaussian wave packets. *Applied Ocean Research*, 10(2):106–108, 1988.

[5] G. F. Clauss. Task-related rogue waves embedded in extreme seas. *Proc. Twenty-First International Conference on Offshore Mechanics and Arctic Engineering*, 2002.

[6] G. F. Clauss and J. Bergmann. Gaussian wave packets - a new approach to seakeeping tests of ocean structures. *Applied Ocean Research*, 10(2):190–206, 1986.

[7] G. F. Clauss and J. Hennig. Deterministic analysis of extreme roll motions using tailored wave sequences. *Proc. Eighth International Conference on the Stability of Ships and Ocean Vehicles*, pages 441–455, 2003.

[8] G. F. Clauss, J. Hennig, and C. E. Schmittner. Modelling extreme wave sequences for the hydrodynamic analysis of ships and offshore structures. *Proc. Practical Design of Ships and Mobile Units (PRADS)*, 2005.

[9] G. F. Clauss, J. Hennig, C. E. Schmittner, and W. L. Kühnlein. Non-linear calculation of tailored wave trains for experimental investigations of extreme structure behaviour. *Proc. Twenty-Third International Conference on Offshore Mechanics and Arctic Engineering*, 2004.

[10] G. F. Clauss and W. L. Kühnlein. Simulation of design storm wave conditions with tailored wave groups. *Proc. First International Offshore and Polar Engineering Conference*, pages 228–237, 1997.

[11] G. F. Clauss and U. Steinhagen. Numerical simulation of nonlinear transient waves and its validation by laboratory data. *Proc. First International Offshore and Polar Engineering Conference*, pages 368–375, 1999.

[12] M. Davis and E. Zarnick. Testing ship models in transient waves. *Proc. Fifth Symposium on Naval Hydrodynamics*, pages 507–543, 1964.

[13] Y.-W. Lee, L. S. McCue, M. S. Obar, and A. W. Troesch. Experimental and numerical investigation into the effects of initial conditions on a three degree of freedom capsize model. *accepted for publication in Journal of Ship Research*, 2004 (accepted).

[14] L. S. McCue and A. W. Troesch. Probabilistic determination of critical wave height for a multi-degree of freedom capsize model. *Ocean Engineering*, 32:1608–1622, 2005.

[15] L. W. Pastoor. *On the Assessment of Nonlinear ship motions and loads.* PhD thesis, Technische Universiteit Delft, 2002.

[16] U. Steinhagen. *Synthesizing Nonlinear Transient Gravity Waves in Random Seas.* PhD thesis, Technische Universität Berlin, 2002.

[17] S. Takezawa and T. Hirayama. Advanced experimental techniques for testing ship models in transient water waves. Part II: The controlled transient water waves for using in ship motion tests. *Proc. Eleventh Symposium on Naval Hydrodynamics*, pages 37–54, 1976.

[18] S. Takezawa and M. Takekawa. Advanced experimental techniques for testing ship models in transient water waves. Part I: The transient test technique on ship motions in waves. *Proc. Eleventh Symposium on Naval Hydrodynamics*, pages 23–35, 1976.

[19] P. H. Taylor, P. Jonathan, and L. A. Harland. Time domain simulation of jack-up dynamics with the extremes of a gaussian process. *Offshore Technology*, 1-A:53–58, 1995.

[20] P. S. Tromans, A. R. Anaturk, and P. Hagemeijer. A new model for the kinematics of large ocean waves - application as a design wave. *Proc. First International Offshore and Polar Engineering Conference*, pages 64–71, 1991.